20th IMEKO TC10 Conference
"Measurement for Diagnostics, Optimization and Control to Support Competitiveness and Innovation"
Lisbon, Portugal, September 28–29, 2026

Testing a Low Processing Methodology for Intermittent Fault Detection in Power Distribution Grids with Low Impedance Neutral

António J. Costa[1*], Hugo Morais[2]

[1]*LNEC, Lisbon, Portugal, ajcosta@lnec.pt*
[2]*INESC-ID, Lisbon, Portugal, hugo.morais@tecnico.ulisboa.pt*

Abstract **– The massive integration of new power generation plants using decentralised renewable energy resources (DER) implies an expansion of the electrical distribution power grid with the construction of more transmission lines and substations. With this expansion, the probability of the occurrence of permanent and intermittent faults will increase.**

The time interval and duration of intermittent faults (IF) vary in time, being characterised by a non-stationary spectrum. Existing algorithms to detect permanent faults may not be effective for the detection of intermittent faults due to the time-varying spectrum characteristics of the latter. The Intelligent Electronic Devices (IEDs) in substations should include new algorithms able to effectively detect intermittent faults. This paper studies and tests the effectiveness of a low-processing time-frequency analysis methodology for detecting intermittent faults in power distribution grids with low-impedance neutral. An analysis over time of the cumulated zero-sequence energy to check for spike persistence is performed. Besides this, a frequency analysis to check the persistence of spectrum peaks around the natural oscillation frequency is also performed. This frequency analysis is important to distinguish from harmonics generated by power electronic converters. Low processing frequency analysis techniques, such as Hilbert Transform (HT) and Derivative Sign Variation (DSV), are adopted. The distribution power grid topology and adopted neutral regime influence the natural frequency of oscillation. A reference distribution grid topology with a high-to-medium voltage distribution transformer and two secondary medium-voltage feeders, one healthy and the other with an intermittent fault, is considered. The grid with a low-impedance neutral using a zigzag (ZZ) transformer for the neutral grounding.

Keywords – Intermittent Faults, Time-Frequency Detection, Zero-Sequence Energy, Hilbert Transform, Derivative Sign Variation.

I. INTRODUCTION

Combined time-frequency analysis should be adopted in the detection of Intermittent faults (IF) because of their stochastic durations and time intervals [1]. With the Short-Time Fourier transform (STFT), the frequency resolution depends on the window analysis period. The continuous wavelet transform (CWT) implies increased processing due to the need to convolve the signal with a set of wavelets defined by different fundamental frequencies [2]. The adopted methodology simultaneously analyses in time the cumulated zero-sequence energy, and in frequency the persistence of zero-sequence current or voltage peaks near the natural oscillation frequency. Techniques requiring low processing in the determination of the almost instantaneous frequency, such as the Hilbert transform (HT) [3], and derivative sign variation (DSV) [4], are considered for the frequency analysis. Previous work has shown that an original version of such low-processing combined time-frequency methodology, based on the analysis of zero-sequence current peaks, enables effective detection of intermittent faults in distribution grids with isolated and high-impedance neutral-to-ground regimes [5]. This paper studies and tests the effectiveness of a modified version of such time-frequency low-processing methodology for detecting intermittent faults in distribution grids with zigzag (ZZ). This modified version is based on the analysis of zero-sequence voltage peaks.

Section II is dedicated to the description of the methodology adopted, algorithms and mathematical formulations. Section III presents the simulated reference distribution grid topology and parameters. Section IV presents and discusses the obtained simulation results. First, the predicted voltage and current evolutions during IF. Then, concerning the detection in time of the zero-sequence cumulative energy. Afterwards, the detection also in frequency of oscillations near the natural frequency using the HT or DSV. A summary of the cut-off and detection times depending on the considered limits is also provided. The effective implementation of selectivity based on faulty and healthy feeder current evolutions is also discussed. Section V presents the main conclusions.

II. METHODOLOGY

A. Intermittent fault modelling

Intermittent faults are characterised by stochastic time intervals and durations. These can be modelled by equation (1), where $u(t)$ is the step function, t_k and δ_k respectively, the beginning instant and duration of each pulse k, and N_p the total number of pulses [6]. The instant t_k for the beginning pulse k is given by the sum of the intervals between all the previous pulses where τ_j is the time interval between the consecutive pulses $j-1$ and j.

$$p(t) = \sum_{k=1}^{N_p} u(t-t_k) - u(t-t_k-\delta_k) \ ; \ t_k = \sum_{j=1}^{k} \tau_j \quad (1)$$

Table 1 states typical pulse durations and time intervals of intermittent faults.

Table 1. Typical durations and intervals of intermittent faults

Duration δ [ms]	Intervals τ [ms]	Ref.
10	90	[3]
10	40, 60, 80, 100, and 160	[7]
10 and 60	100	[8]
10	40, 60, 100, 120, 140, 280, and 400	[9]

Variables τ_j and δ_k can be considered stochastic with Gaussian distributions. If τ_j Gaussian with a mean value $\mu_\tau = 100$ ms and standard deviation $\sigma_\tau = 20$ ms, 99.7% of the pulses are generated with time intervals between 40 ms and 160 ms. If δ_k Gaussian with a mean value $\mu_\delta = 10$ ms and $\sigma_\delta = 2$ ms, 99.7% of the pulses are generated with durations between 4 ms and 16 ms.

B. IF detection algorithm and formulations

The algorithm for combined time-frequency detection of intermittent faults is shown in Fig. 1. The first condition consists of verifying if the zero-sequence energy E_0 calculated by (2), where U_0, I_0 and $P_{0_{ef}}$ are respectively the zero-sequence voltage, current and effective power, exceeds a given maximum allowable value $E_{0_{max}}$.

$$E_0(t) = \int_0^t P_{0_{ef}}(\tau)\, d\tau \quad ; \quad P_{0_{ef}} = \sqrt{\langle {U_0}^2\, {I_0}^2 \rangle_T} \quad (2)$$

The second condition consists of verifying if the number of spectrum peaks n_f, near the natural oscillation frequency with minimum and maximum limiting frequencies f_{min} and f_{max} , exceeds a given limit $n_{f_{max}}$.
Two techniques requiring low processing for quasi-instantaneous frequency detection of the real-time function $r(t)$, are tested: i) Hilbert Transform (HT), and ii) Derivative Sign Variation (DSV).
In the first technique, the frequency is determined from the phase variation using (3), where $H\{r(t)\}$ is the HT of $r(t)$ given by (4).

$$f = \frac{1}{2\pi}\frac{d\phi(t)}{dt} \quad ; \quad \phi(t) = atan\left(\frac{H\{r(t)\}}{r(t)}\right) \quad (3)$$

$$H\{r(t)\} = r(t) * \frac{1}{\pi\, t} = \frac{1}{\pi}\int_{-\infty}^{+\infty} \frac{r(t-\tau)}{\tau}\, d\tau \quad (4)$$

The second technique consists of calculating the derivative of I_0 or U_0 and verifying the instants when the derivative sign changes. The instantaneous frequency is calculated by the reciprocal of the difference between two successive instants when $sign\,(d\,I_0/dt)$ changes from negative to positive or vice versa.

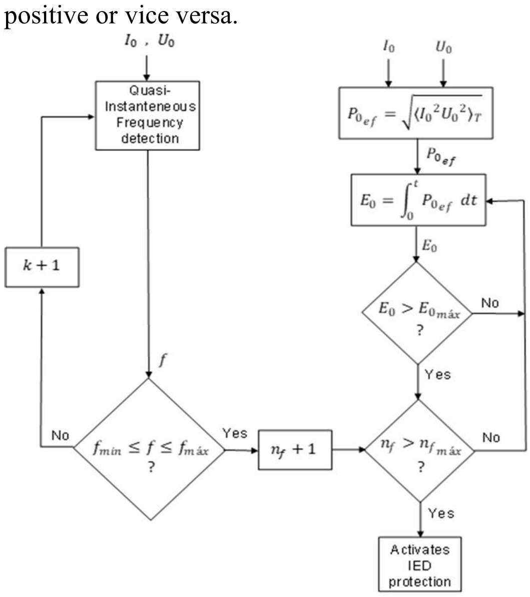

Fig. 1. Algorithm for detection of intermittent faults.

III. SIMULATED REFERENCE GRID TOPOLOGY AND PARAMETERS

The simulated reference distribution grid topology includes a distribution Y/D transformer with the primary coil connected to a high voltage (HV) line at 60 kV, with 3.5 km length, and the secondary coil connected to two medium voltage (MV) feeders at 15 kV, with 25 km length, supplying inductive loads consuming 10 kVar of reactive power.
Fig. 2 shows the single-line diagram of the reference distribution grid with zigzag (ZZ) grounding neutral [10].

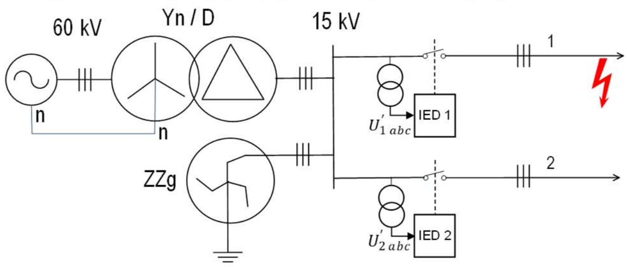

Fig. 2. Single-line diagram of the reference distribution grid with ZZ grounding neutral.

Fig. 3 shows the corresponding the Simulink diagram of the reference distribution grid with ZZ grounding neutral.

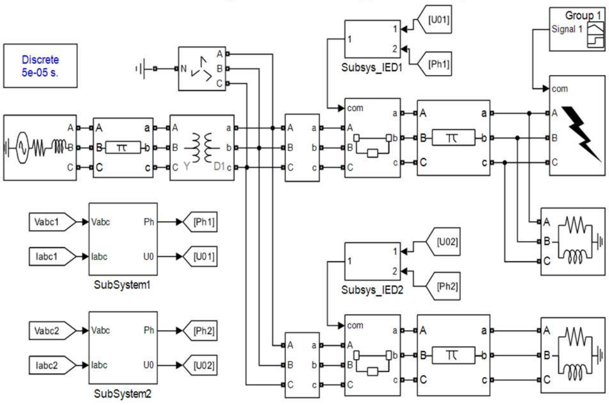

Fig. 3. Simulink diagram of the reference distribution grid with ZZ grounding neutral.

A Phase-to-Ground fault was established in one of the MV feeders at the terminal load connection bus.

IV. PRESENTATION AND DISCUSSION OF RESULTS

This section presents simulation results of the faulty phase and zero-sequence voltage, current, and power evolutions during the phase-to-ground intermittent fault (IF) with the ZZ neutral grounding. First, the evolution under no protection. Then with cut-off based on b) time detection of the zero-sequence cumulative energy, and combined time-frequency detection using the c) HT or d) DSV.

A. Zero-Sequence Voltage and Current during IF

Fig. 4 shows the evolution of the faulty phase voltage U_a and current I_a under a series of pulses $p(t)$ triggering phase-to-ground intermittent faults (IF), with the ZZ neutral grounding. Fig. 5 shows the evolution of the zero-sequence voltage U_0, current I_0, and power P_0, under no cut-off protection. The detailed evolutions of U_0, I_0, and P_0 from $t = 0.9$ s to 1 s is presented in Fig. 6.

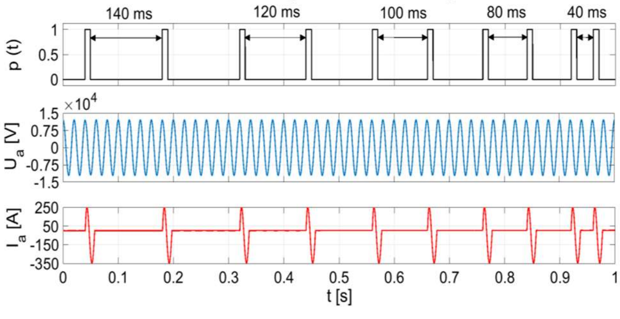

Fig. 4. Evolution of the faulty U_a, I_a, during 1 s with no cut-off.

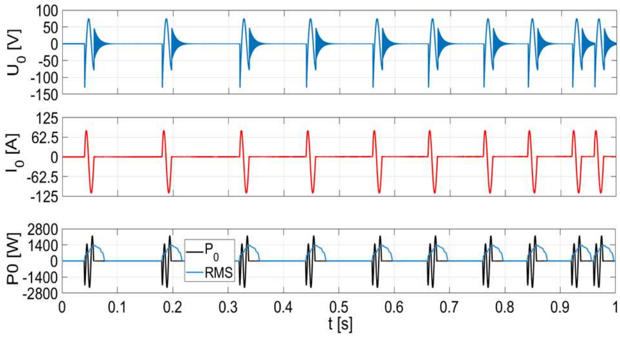

Fig. 5. Evolution of U_0, I_0, and P_0 during 1 s with no cut-off.

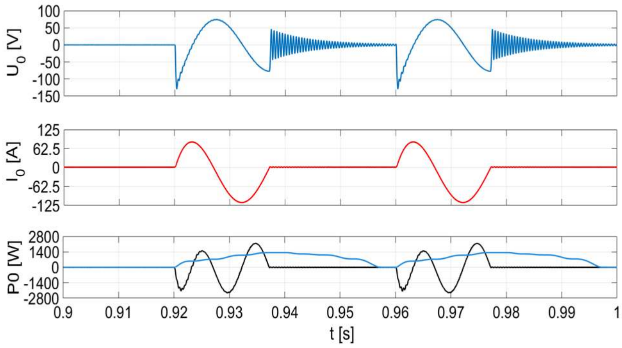

Fig. 6. Evolution of U_0, I_0, and P_0 during the last 0.1 s.

The root-mean-square power $P_{0_{ef}}$ is the dotted blue line. With the ZZ grounding neutral, 22 oscillations of U_0 occurred during 10 ms, giving a natural oscillation frequency of $f_n \approx 2200$ Hz.

B. Time detection of zero-sequence cumulative energy

This subsection presents results from the time detection of zero-sequence cumulative energy. Fig. 7 and Fig. 8 show the IED cut-off instants with $E_{0_{max}}$ equal to 10 J and 100 J.

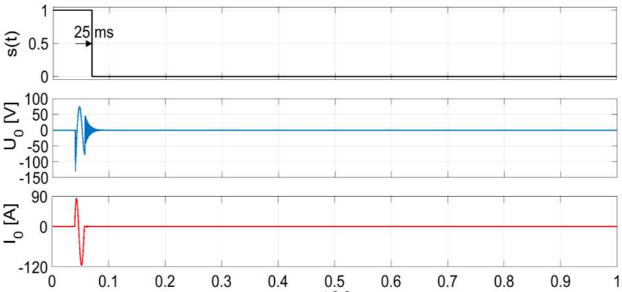

Fig. 7. IED cut-off for $E_{0_{max}} = 10$ J.

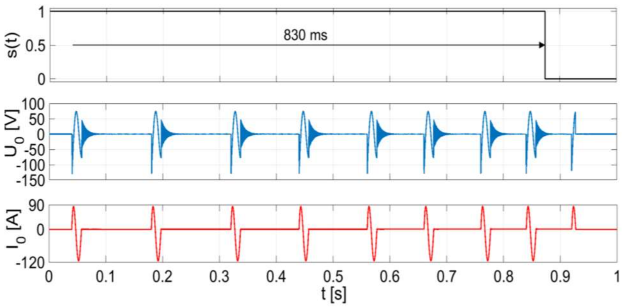

Fig. 8. IED cut-off for $E_{0_{max}} = 100\,J$,

With the ZZ grounding neutral, the verified IED cut-off time τ_{off} was about 25 ms for $E_{0_{max}} = 10$ J, actuating just after the beginning of the first pulse, and about $\tau_{off} \approx$ 830 ms for $E_{0_{max}} = 100$ J.

C. Combined Time-Frequency using Hilbert Transform

In the combined time-frequency analysis, the IED cut-off is performed when exceeding $E_{0_{max}}$, and the number n_f of spectrum peaks between f_{min} and f_{max} exceeds $n_{f_{max}}$. This subsection presents results from combined time-frequency detection using HT. The Simulink block diagram for low-processing frequency detection using the HT is shown in Fig. 9.

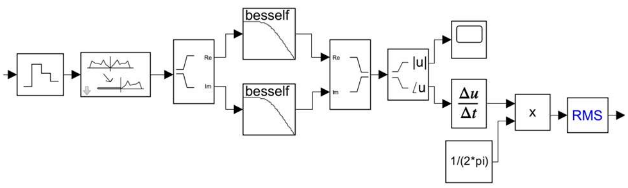

Fig. 9. Simulink diagram for frequency detection using HT.

Fig. 10 shows the U_0 frequency evolution obtained from HT. A lower frequency limit $f_{min} = 1500$ Hz was considered.

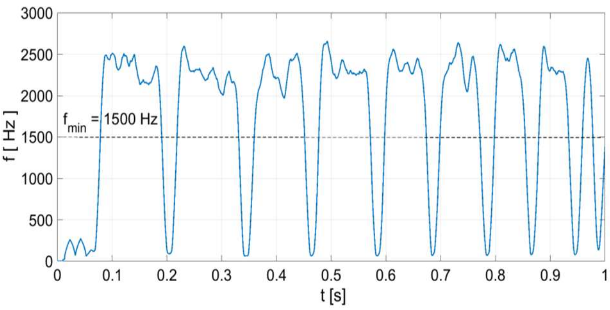

Fig. 10. Evolution of the U_0 frequency from HT.

Fig. 11 shows the evolution of U_0 and I_0 with IED cut-off based on combined time-frequency detection with $E_{0_{max}} = 10$ J and $n_{f_{max}} = 3$. The predicted IED cut-off time was $\tau_{off} \approx 375$ ms. The predicted detection time after counting $n_{f_{max}} = 3$ was $\tau_d \approx 94$ ms.

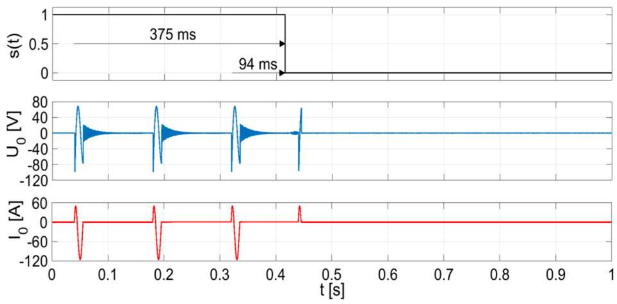

Fig. 11. Cut-off for $E_{0_{max}} = 10\,J$ and $n_{f_{max}} = 3$ using HT.

Fig. 12 refers to the case with $E_{0_{max}} = 10$ J and $n_{f_{max}} = 6$. In this case, the predicted IED cut-off time was $\tau_{off} \approx 662$ ms. The predicted detection time after counting $n_{f_{max}} = 6$ was $\tau_d \approx 42$ ms.

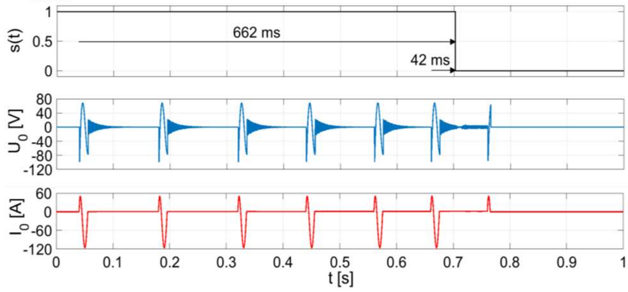

Fig. 12. Cut-off for $E_{0_{max}} = 10\,J$ and $n_{f_{max}} = 6$ using HT.

D. Combined Time-Frequency using Derivative Variation

The Simulink block diagram for low processing frequency detection using the DSV is shown in Fig. 13.

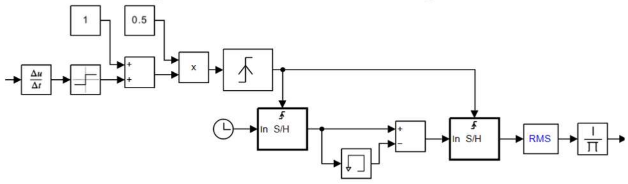

Fig. 13. Simulink diagram for frequency detection using DSV.

Fig. 14 shows the U_0 frequency evolution obtained from DSV. A lower frequency limit of $f_{min} = 1500$ Hz.

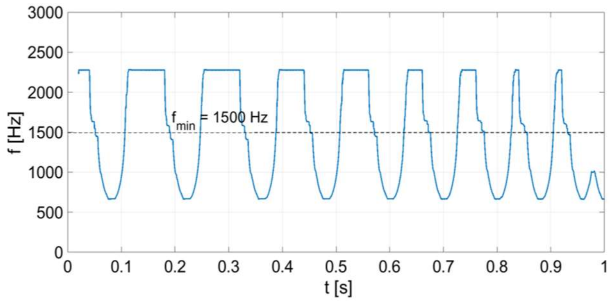

Fig. 14. Evolution of U_0 frequency from DSV.

Fig. 15 shows the evolution of U_0 and I_0 with IED cut-off based on combined time-frequency detection with

$E_{0_{max}} = 10$ J and $n_{f_{max}} = 3$. The predicted IED cut-off time was $\tau_{off} \approx 345$ ms. The predicted detection time after counting $n_{f_{max}} = 3$ was $\tau_d \approx 64$ ms.

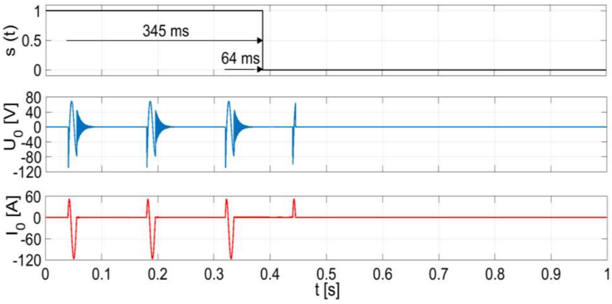

Fig. 15. Cut-off for $E_{0_{max}} = 10\,J$ and $n_{f_{max}} = 3$ using DSV.

Fig. 16 refers to the case with $E_{0_{max}} = 10$ J and $n_{f_{max}} = 6$. In this case the predicted IED cut-off time was $\tau_{off} \approx 680$ ms. The predicted detection time after counting $n_{f_{max}} = 6$ was $\tau_d \approx 60$ ms.

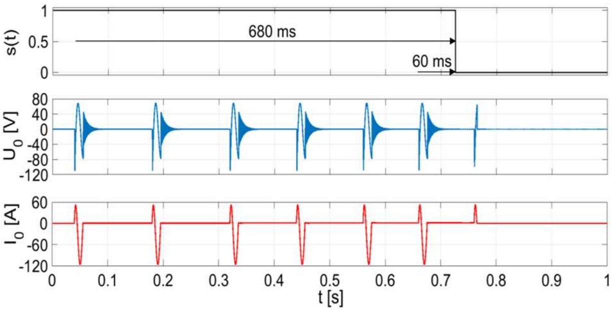

Fig. 16. Cut-off for $E_{0_{max}} = 10\,J$ and $n_{f_{max}} = 6$ using DSV.

E. Overview of cut-off and detection times

An overview of the obtained cut-off times τ_{off} and detection times τ_d, depending on the applied detection technique and considered limits $E_{0_{max}}$ or $n_{f_{max}}$ are stated in Table 2. The τ_{off} refers to the time of cut-off from the beginning of the initial fault in the intermittent sequence. The τ_d is the detection time till the cut-off after counting the maximum number of spectrum peaks near the natural oscillation frequency. This detection time is considered when applying the HT or DSV. It depends on the distribution grid natural oscillation frequency and on the combined time-frequency detection technique.

Table 2. Overview of obtained cut-off and response times

Time $E_{0_{max}}$ [J]	Frequency $n_{f_{max}}$ [1]	τ_{off} [ms]	τ_d [ms]
10	-	25	-
100	-	830	-
10	HT ; #3	375	94
10	HT ; #6	662	42
10	DSV ; #3	345	64
10	DSV ; #6	680	60

In the time-detection of the zero-sequence cumulative energy, the cut-off time τ_{off} increases with the maximum allowable cumulative energy limit $E_{0_{max}}$, as expected. Both the HT and DSV frequency detection techniques presented similar cut-off times for the same maximum number of spectrum peaks near the natural oscillation frequency. The predicted τ_{off} was in average 360 ms with $n_{f_{max}} = 3$, and 671 ms with $n_{f_{max}} = 6$. The predicted detection time τ_d was in average 68 ms using the HT and 62 ms using the DSV frequency detection. Simulations were done for the combined time-frequency also with $E_{0_{max}} = 100$ J. In this case, the obtained cut-off time was $\tau_{off} = 830$ ms demonstrating that the used algorithm responds only when both the $E_{0_{max}}$ and $n_{f_{max}}$ limits are verified, showing its time-frequency detection robustness.

F. Selectivity from faulty and healthy current evolutions

The current evolutions during the IF, on all the faulty and healthy feeder phases, were analysed. Fig. 17 shows for the phase-to-ground short-circuited phase (a), the evolutions of the voltage U_a, the current in the faulty feeder I_{a_f}, and the current in the healthy feeder I_{a_h}. The root of the mean squared (RMS) values are the dotted lines.

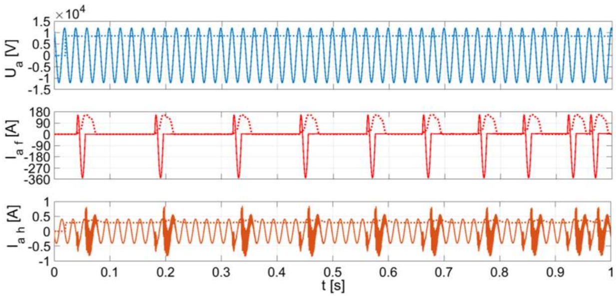

Fig. 17. Evolutions of U_a, I_{a_f} and I_{a_h}.

The RMS of I_{a_f} returns to zero during periods between consecutive faults. The RMS of I_{a_h} is always greater than zero. This is also true for the currents in the non-short-circuited phases (b) and (c) of the faulty and healthy feeders. So, one effective way to distinguish between the faulty and heathy feeders is to monitor the RMS value of the currents in all phases. If there are periods with a current RMS nearly zero, the corresponding phase has an earth-to-ground short-circuit. This detection is more properly done, looking for the charge (integral of the current RMS) evolutions. Fig. 18 shows the charge evolutions of phase (a) Q_{a_f} and Q_{a_h} respectively in the faulty and healthy feeders.

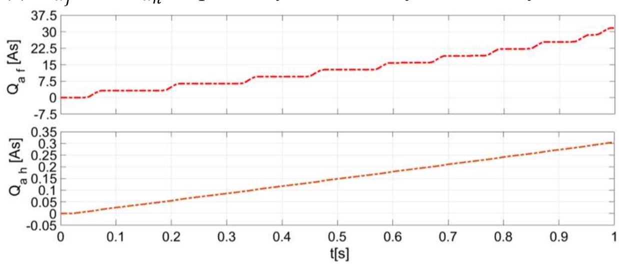

Fig. 18. Evolutions of Q_{a_f} and Q_{a_h}.

Q_{a_f} remains constant during periods between faults while Q_{a_h} is always increasing.

V. CONCLUSION

A modification was made in the considered low processing combined time-frequency methodology, performing the analysis of zero-sequence voltage peaks instead of zero-sequence current peaks to enable effective detection of intermittent faults with the low impedance neutral grounding. Simulation results have shown that the modified methodology responds at proper cut-off timings given a maximum allowable zero-sequence energy and number of spectrum peaks.

Similar cut-off times were obtained using both the Hilbert Transform (HT) and Derivative Sign Variation (DSV) frequency detection techniques, considering the same value for the maximum allowable number of spectrum peaks near the natural oscillation frequency. The predicted response cut-off time was, on average, the same using both HT and DSV. The predicted average value was on average 65 ms for the considered reference distribution grid topology and Zig-Zag neutral regime.

An effective way to implement selectivity is to measure the root of the mean squared (RMS) value of the currents on all phases. When the current RMS assumes zero, or the corresponding integral in time (charge) is constant, during periods between consecutive faults, the corresponding line has an earth-to-ground short-circuit and the associated faulty feeder should be isolated from the remaining distribution grid.

VI. ACKNOWLEDGMENTS

This research was funded by project nº 56 - "*Aliança para a Transição Energética*", financed by Recovery and Resilience Plan (PRR) - Component 5, included in the NextGenerationEU funding program and supported by FCT, under project UIDB/50021/2020.

REFERENCES

[1] **Z. Gajić, S. Zubić, M. Kockott:** Phasor-Based Transient Earth-Fault Protection, *74th Conference for Protective Relay Engineers (CPRE)*, pp. 1–26, 2021.

[2] **D. Zhou, Y. Zhao, Z. Wang, X. He, M. Gao,** Review on Diagnosis Techniques for Intermittent Faults in Dynamic Systems, *IEEE Trans. Ind. Electron.,* vol. 67, n.º 3, pp. 2337–2347, 2020.

[3] **T. Cui, X. Dong, Z. Bo, A. Juszczyk:** Hilbert-Transform-Based Transient/Intermittent Earth Fault Detection in Noneffectively Grounded Distribution Systems *IEEE Trans. Power Deliv.*, vol. 26, n.º 1, pp. 143–151, 2011.

[4] **Y. Abdoush, J. A. Garcia-Molina, G. E. Corazza:** Adaptive instantaneous frequency estimation based on time-frequency distributions with derivative approximation, *Signal Process.*, vol. 160, pp. 99–105, 2019.

[5] **A. A. Costa, P. Carvalho, A. Aleixo, J. Peres, R. D. Jorge, and Hugo Morais:** Algorithms for intermittent fault detection with high-impedance neutral-to-ground regimes, *IET-proceedings of the CIRED 28th International Conference and Exhibition on Electricity Distribution,* vol. 2025, nº. 14, 2025.

[6] **K. Zhang, B. Gou, W. Xiong, X. Feng:** An Online Diagnosis Method for Sensor Intermittent Fault Based on Data-Driven Model, *IEEE Trans. Power Electron.*, vol. 38, n.º 3, pp. 2861–2865, 2023.

[7] **J. Altonen, O. Mäkinen, K. Kauhaniemi, K. Persson:** Intermittent Earth Faults-Need to Improve the Existing Feeder Earth Fault Protection Schemes?, *CIRED, 17th International Conference on Electricity Distribution*, 2003.

[8] **M. Hojabri, S. Nowak, A. Papaemmanouil:** ML-Based Intermittent Fault Detection, Classification, and Branch Identification in a Distribution Network. *Energies*, vol. 16, n.º 16, Art. n.º 16, 2023.

[9] **K. Łowczowski, B. Olejnik:** Monitoring, Detection and Locating of Transient Earth Fault Using Zero-Sequence Current and Cable Screen Earthing Current in Medium Voltage Cable and Mixed Feeders. *Energies*, 15(3), 2022.

[10] **R. Cimadevilla, A. García, J. Á. G. Viosca, e C. A. Domínguez:** Protection of MV networks using zig-zag grounding transformers, *19th IET Conference on Developments in Power System Protection (DPSP Europe 2025),* pp. 201–210, April 2025.